Can. J. Remote Sensing, Vol. 30, No. 6, pp. 903–912, 2004

Comparison of clear-sky surface radiative fluxes simulated with radiative transfer models

E. Puckrin, W.F.J. Evans, J. Li, and H. Lavoie

Abstract. The surface fluxes of several important radiatively active gases, including H_2O, CO_2, CH_4, N_2O, O_3, and the chlorofluorocarbons CFC11 and CFC12, were simulated with the radiation band models from the National Center for Atmospheric Research (NCAR) community climate model 3 (CCM3), the single-column community atmospheric model (SCAM), and the Canadian global climate model 3 (GCM3). These results were compared with the measured fluxes for a very cold winter day and with the simulated results for other standard atmospheres using the line-by-line radiative transfer model (LBLRTM). The comparison shows that the total surface radiative flux contributed by all the greenhouse gases combined is well simulated by the SCAM and GCM3 radiation band models. The two models generally agree within about 1% of the line-by-line result for all the atmospheric conditions studied. The error in the total flux simulated by the older CCM3 code, however, can be as large as 7% depending on the atmospheric conditions. The SCAM code consistently models H_2O better than the CCM3 and GCM3 codes, typically displaying errors of less than 1 W/m^2 for all atmospheric conditions. All of the models have difficulty in modelling accurately the radiative flux of CH_4 and N_2O. In general, the inaccuracy increases, by as much as 200% in some cases, as the amount of H_2O in the atmosphere increases. The source of the problem appears to be related to the overlapping bands of other gases. The error in the ozone flux varies from 5% to 15% for the CCM3 and SCAM models, and it can be as large as 30% for the GCM3 code. The CCM3 and SCAM models simulated the chlorofluorocarbon fluxes to within 0.06 W/m^2, but this leads to relative errors of 20%–40% for the various atmospheric scenarios. The errors for the CFCs are even larger in the case of the GCM3 model.

Résumé. Les flux de surface de plusieurs gaz actifs importants au plan radiatif, incluant H_2O, CO_2, CH_4, N_2O, O_3 et les chlorofluorocarbures CFC11 et CFC12, ont été simulés à l'aide des modèles de transfert radiatif à bande étroite CCM3 (« NCAR community climate model 3 »), SCAM (« single-column community atmospheric model ») et GCM3 (« Canadian global climate model 3 »). Ces résultats ont été comparés aux flux mesurés pour une journée très froide d'hiver et aux résultats de simulation pour d'autres atmosphères standard utilisant le modèle de transfert radiatif raie par raie LBLRTM (« line-by-line radiative transfer model »). La comparaison montre que le flux radiatif total de surface résultant de l'effet combiné de tous les gaz à effet de serre est bien simulé par les modèles de transfert radiatif SCAM et GCM3. Les deux modèles sont généralement en accord à l'intérieur de 1 % par rapport au résultat obtenu avec le modèle raie par raie pour toutes les conditions atmosphériques étudiées. Toutefois, l'erreur dans le flux total simulé à l'aide du code plus ancien CCM3 peut être aussi élevée que 7 % selon les conditions atmosphériques. Le code SCAM modélise mieux et de façon plus constante H_2O que les codes CCM3 et GCM3, affichant typiquement des erreurs de moins de 1 W/m^2 pour toutes les conditions atmosphériques. Tous les modèles ont de la difficulté à modéliser de façon précise le flux radiatif de CH_4 et N_2O. En général, l'imprécision augmente, jusqu'à 200 % dans certains cas, en fonction de l'accroissement de H_2O dans l'atmosphère. La source du problème semble être reliée au phénomène de la superposition des bandes des autres gaz. L'erreur dans le flux de l'ozone varie de 5 %–15 %, pour les modèles CCM3 et SCAM, et peut être aussi considérable que 30 % dans le cas du code GCM3. Les modèles CCM3 et SCAM simulent les flux de chlorofluorocarbures à l'intérieur de 0.06 W/m^2, mais ceci entraîne des erreurs relatives de 20 %–40 % pour les divers scénarios atmosphériques. Les erreurs au niveau des CFC sont encore plus grandes dans le cas du modèle GCM3.
[Traduit par la Rédaction]

Introduction

Climate models of varying complexity have been used for many years to evaluate the impact of anthropogenic and natural perturbations on the climate system. The most complex of these models include the three-dimensional, coupled atmosphere–ocean general circulation models (GCMs). As a result of the degree of model complexity, simplifying assumptions must be made to reduce their computational requirements. This includes simplifying the radiation schemes within the GCMs; many different approaches can be used by the models, and it is important to identify and understand how these differences and the simplifying assumptions in the radiation codes affect model sensitivity.

To address this problem, the program for the intercomparison of radiation codes used in climate models (ICRCCM) was

Received 17 June 2003. Accepted 9 June 2004.

E. Puckrin[1] and H. Lavoie. Defence R&D Canada – Valcartier, Val-Belair, QC G3A 1X5, Canada.

W.F.J. Evans. Physics Department, Trent University, Peterborough, ON K9J 7B8, Canada.

J. Li. Canadian Centre for Climate Modelling and Analysis, Victoria, BC V8W 2Y2, Canada.

[1]Corresponding author (e-mail: eldon.puckrin@drdc-rddc.gc.ca).

established several years ago. One of the first ICRCCM intermodel comparisons showed that for the case of clear-sky longwave fluxes, the various radiation codes exhibited relatively large differences of 10%–20% (Luther et al., 1988; Ellingson et al., 1991). The level of disagreement was larger for single absorbing gas atmospheres, whereas cases that included complete atmospheres showed better agreement. Since the time of the first model comparison, there have been changes incorporated in the radiation codes to increase their accuracy and the level of agreement with other codes. Many laboratories have been actively comparing model results in an effort to validate the newer versions of these models.

Hence, the focus of this paper is to compare the clear-sky longwave fluxes at the surface as simulated by three popular climate models with the results of an accurate line-by-line code. Specifically, the column radiation models (CRMs) incorporated in the National Center for Atmospheric Research (NCAR) community climate model 3 (CCM3), the single-column community atmospheric model (SCAM), and the Canadian global climate model 3 (GCM3) were used to predict the clear-sky radiative fluxes associated with a number of important greenhouse gases, including water vapour (H_2O), carbon dioxide (CO_2), methane (CH_4), nitrous oxide (N_2O), ozone (O_3), and the chlorofluorocarbons CFC11 and CFC12. The simulations were performed for five different atmospheric conditions: (*i*) the very cold winter conditions of 16 February 1996, for which measured radiative fluxes exist; (*ii*) typical mid-latitude winter (MLW) conditions; (*iii*) average global conditions that are characterized by the 1976 United States standard (USS) atmosphere; (*iv*) typical mid-latitude summer (MLS) conditions; and (*v*) typical tropical conditions. The four latter atmospheres were based on the atmospheric constituent profiles from the US Air Force Geophysics Laboratory (Anderson et al., 1986). The temperature, humidity, and O_3 profiles for these five atmospheres are presented in **Figures 1** and **2**. The cold winter conditions that were present on 16 February 1996 resulted in a minimal amount of H_2O in the atmosphere. The MLW profile provides a scenario in which there is about three times more H_2O in the atmosphere than in the case for 16 February 1996. Average global conditions have been simulated with the 1976 USS atmospheric profile, which is characterized by the autumn conditions present at latitude 30°N. This atmosphere contains about one and a half times more H_2O than the previous scenario representing the MLW conditions. The MLS conditions consist of an atmosphere that contains twice as much H_2O as in the USS atmosphere. The tropical atmosphere contains about one and a half times more H_2O than the MLS profile and about 14 times more H_2O than the cold winter conditions of 16 February 1996.

The simulated results from the NCAR CCM3 and SCAM radiation models and the Canadian GCM3 radiation model were compared with measurements and simulations computed with the line-by-line radiative transfer model LBLRTM (Clough and Iacono, 1995). This model has been extensively validated previously with measurements in the thermal infrared (e.g., Wang et al., 1996; Philipona et al., 2001; Shephard et al., 2003). Such comparisons as detailed here are useful and necessary to verify the calculation of the radiative fluxes from greenhouse gases by radiation models in current GCMs.

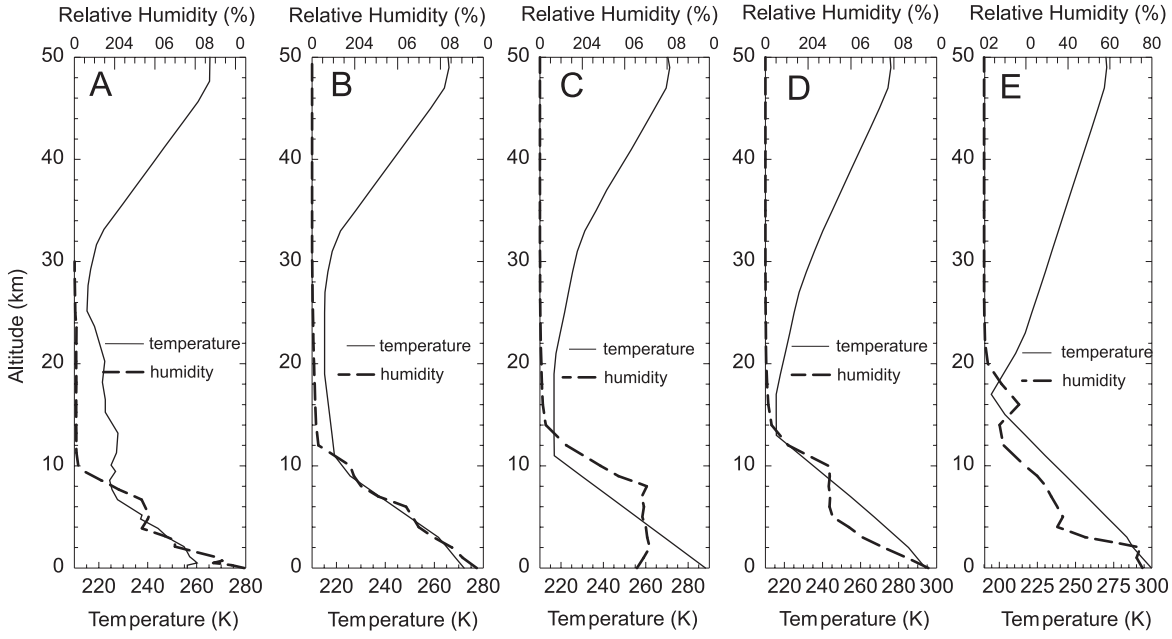

Figure 1. Atmospheric profiles of temperature and relative humidity for (A) cold winter conditions of 16 February 1996, (B) mid-latitude winter conditions, (C) average global conditions, (D) mid-latitude summer conditions, and (E) tropical conditions. Radiative fluxes were modelled using all five of these profiles in the CRMs and the LBLRTM line-by-line code.

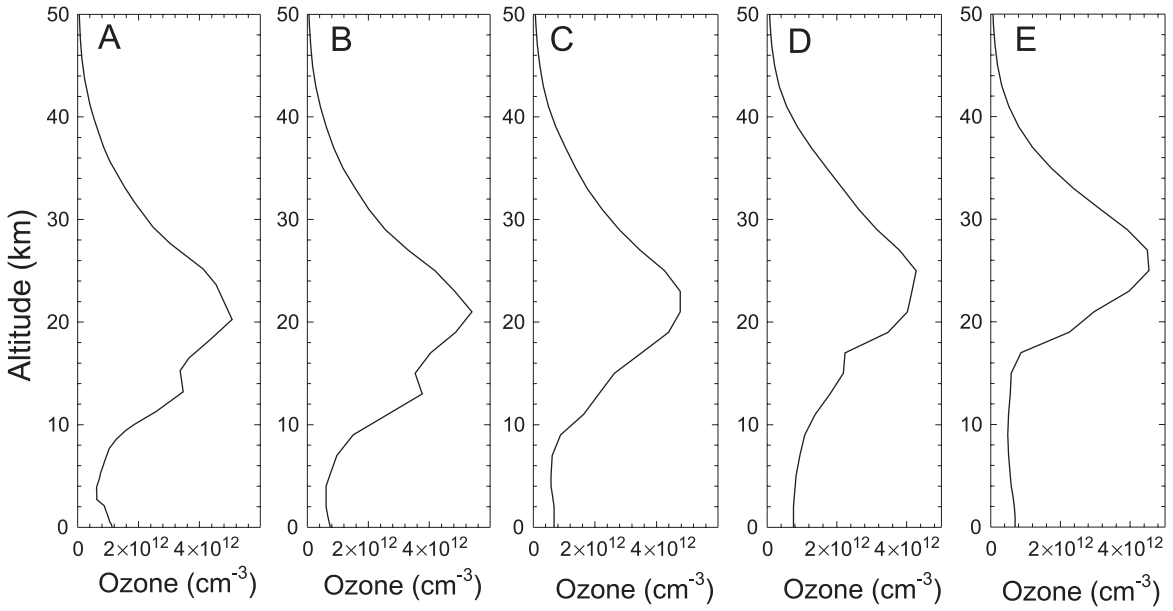

Figure 2. Ozone profiles for (A) cold winter conditions of 16 February 1996, (B) mid-latitude winter conditions, (C) average global conditions, (D) mid-latitude summer conditions, and (E) tropical conditions. Ozone radiative fluxes were modelled using all five of these profiles in the CRMs and the LBLRTM line-by-line code.

Methodology of flux simulations

The radiative flux for a particular gas was calculated with each column radiation model by first simulating the downward surface flux with all gases present and then recalculating the surface flux with the concentration of the particular gas set to zero. In the case of water, both the vapour and continuum were set to zero. Exactly the same atmospheric profile was used for all the models, which consisted of 40 levels from the surface to 100 km. The concentrations of the greenhouse gases used in the study are summarized in **Table 1**. The gas concentrations were held constant throughout the atmosphere (from 0 to 100 km) for CO_2, CH_4, N_2O, and the chlorofluorocarbons. The temperature, H_2O, and O_3 profiles were variable, and they are represented in **Figures 1** and **2**, respectively. The temperature and relative humidity data for 16 February 1996 were obtained from a radiosonde launched at the time of the radiative flux measurements. The corresponding O_3 profile was obtained by slightly altering the mid-latitude profile in the LBLRTM model until agreement was achieved with the measured O_3 intensity.

The reference fluxes calculated with the LBLRTM model (version 8.3) were computed in a similar way; however, the flux was derived by first simulating the downward radiance for six zenith angles (0, 30°, 60°, 70°, 80°, and 85°). The resulting splined radiance curve was integrated over the full sky to obtain the flux value. Decreasing the interval between angles to just 5° altered the calculated fluxes by less than 0.01 W/m^2; hence, the six angles were sufficient for determining the flux value. The LBLRTM model incorporated the MT_CKD_1.00 H_2O continuum model (Mlawer et al.[2]) and the line parameters from the HITRAN 2000 database (Rothman et al., 2003). The radiative effects from aerosols and clouds were not included in any of the model simulations.

Table 1. Constituent amounts used in the model comparisons.

Constituent	Concentration
H_2O	See **Figure 1**
CO_2	360 ppmv
CH_4	1.6 ppmv
N_2O	0.3 ppmv
O_3	See **Figure 2**
CFC11	280 pptv
CFC12	530 pptv
Aerosol	None

Note: ppmv and pptv, parts per million and parts per thousand by volume.

Column radiation models in this study

Column radiation model of GCM3

The Canadian GCM3 model has been used extensively in climate prediction (e.g., Arora and Boer, 2001; 2002). The CRM of the Canadian GCM3 climate model is based on the code by Morcrette (1991). The calculation of the clear-sky longwave flux is similar to that as performed in the older

[2] M.J. Mlawer, D.C. Tobin, and S.A. Clough. A revised perspective on the water vapor continuum: the MT_CKD model. *Journal of Quantitative Spectroscopy and Radiative Transfer*. In preparation.

version GCM2 model, where there are six radiation bands that cover the spectral range from 0 to 2820 cm^{-1} (**Table 2**). The radiation code in the GCM3 model includes an improved treatment of the broadband emissivities and of the H_2O continuum that replaces the parameterization of Roberts et al. (1976) for the H_2O continuum in GCM2. The new parameterization of the H_2O continuum, developed by Clough et al. (1989), is based on line-by-line calculations. This parameterization includes the effect of the H_2O contribution throughout the complete infrared band region, which is an improvement on the parameterization of Roberts et al. that was mostly restricted to the transparent window region. It has been shown that this parameterization is necessary and has considerable influence on the longwave-cooling rate (Clough et al., 1992; Zhong and Haigh, 1995). To implement the parameterization, band 2 in the radiation code has been split into two intervals 500–650 and 650–800 cm^{-1}. Also, band 3 has been calculated separately for the two intervals 800–970 and 1110–1250 cm^{-1}. In addition, the transmission data for both the lines and continuum of H_2O have been updated. It was also found that one band including the 800–970 and 1110–1250 cm^{-1} regions for N_2O was missed in the earlier GCM2 model. This band can result in a significant difference in the calculation of the longwave flux, and its inclusion results in less cooling in the lower troposphere.

Column radiation model of CCM3 and SCAM

The CRM of CCM3 used in this comparison is a stand-alone version (crm-2.1.2-ccm-3.6) of the radiation model provided by the NCAR community (Kiehl et al., 1996). It has been used extensively to study the earth's energy budget and the radiative forcing of greenhouse gases and aerosols (e.g., Kiehl et al., 1998). The radiative transfer of the CRM is based on an absorptivity–emissivity formulation of Ramanathan and Downey (1986). The line parameters are determined in a process that uses an early version of the HITRAN spectroscopic database (Kiehl and Ramanathan, 1983). The longwave radiation extends from 0 to 2200 cm^{-1}, and the interval between 500 and 1500 cm^{-1} is divided into eight bands, as summarized in **Table 3**, to calculate the trace gas absorption. Complete details concerning the band parameterizations are given by Kiehl et al. (1996).

The most recent climate model developed by NCAR is the community atmospheric model 2 (CAM2). It is based on the older CCM3; however, the radiation parameterization of CAM2 differs significantly from that of the CCM3 model. In addition, the CRM of CAM2 benefits from a substantially updated treatment of H_2O emission and absorption, which is based on the 1996 HITRAN database (Rothman et al., 1998) and the CKD continuum model version 2.1 (Clough et al., 1989). In the present work, the single-column version (SCAM) of CAM2 was used to simulate the radiative fluxes. Further details concerning the parameterization of the SCAM code are given by Collins et al. (2002).

Results and discussion

Representative thermal emission bands for the gases investigated in this study are shown in **Figures 3–9** for the two extreme atmospheric scenarios consisting of the cold, dry winter profile of 16 February 1996 and the warm, moist conditions of the tropical atmosphere. All of these spectra have been simulated for the zenith geometry using the LBLRTM model. Most of the molecules have one or two isolated bands; however, **Figure 3** shows that numerous bands of H_2O exist throughout the entire thermal infrared region. Clearly, the H_2O dominates the terrestrial emission as the atmospheric

Table 2. Radiation bands of the Canadian GCM3 radiation model.

Band No.	Spectral region (cm^{-1})
1	0–350, 1450–1880
2	500–650, 650–800
3	800–970, 1110–1250
4	970–1110
5	350–500
6	1250–1450, 1880–2820

Table 3. Radiation bands of the NCAR CCM3 and SCAM radiation models.

Band No.	Spectral region (cm^{-1})
1	500–750
2	750–820
3	820–880
4	880–900
5	900–1000
6	1000–1120
7	1120–1170
8	1170–1500

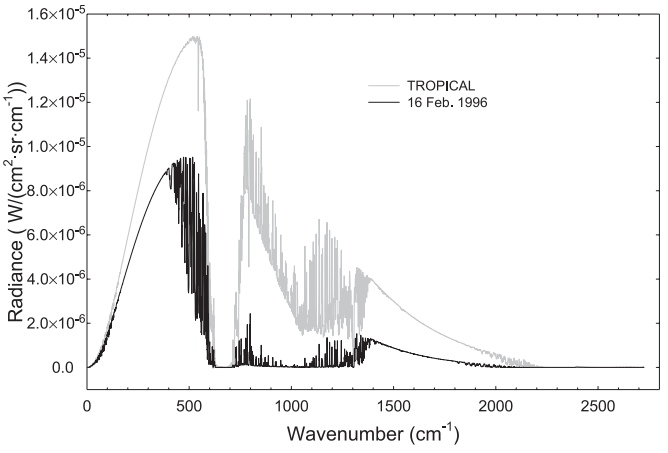

Figure 3. LBLRTM simulations of the downward H_2O radiance at the surface for two extreme atmospheric scenarios: the cold winter conditions of 16 February 1996, and the warm, humid atmosphere of tropical conditions.

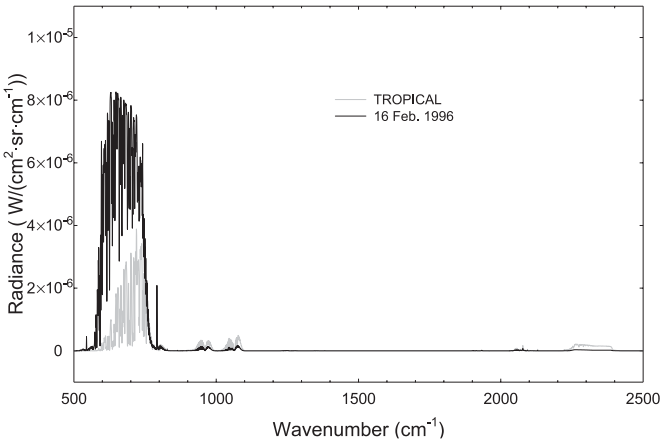

Figure 4. LBLRTM simulations of the downward CO_2 radiance at the surface for two extreme atmospheric scenarios: the cold winter conditions of 16 February 1996, and the warm, humid atmosphere of tropical conditions.

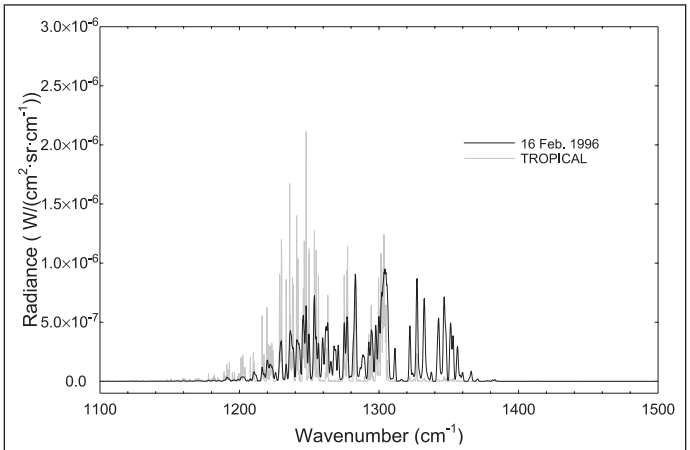

Figure 5. LBLRTM simulations of the downward CH_4 radiance at the surface for two extreme atmospheric scenarios: the cold winter conditions of 16 February 1996, and the warm, humid atmosphere of tropical conditions.

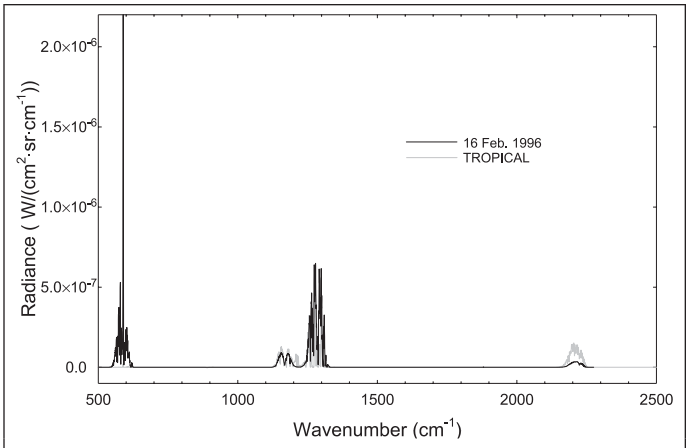

Figure 6. LBLRTM simulations of the downward N_2O radiance at the surface for two extreme atmospheric scenarios: the cold winter conditions of 16 February 1996, and the warm, humid atmosphere of tropical conditions.

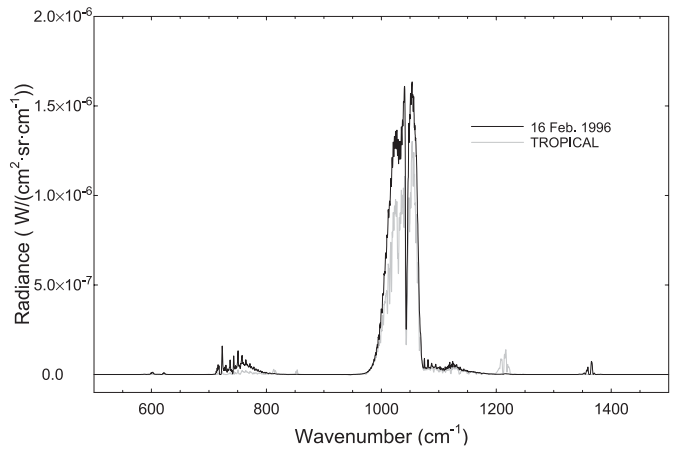

Figure 7. LBLRTM simulations of the downward O_3 radiance at the surface for two extreme atmospheric scenarios: the cold winter conditions of 16 February 1996, and the warm, humid atmosphere of tropical conditions.

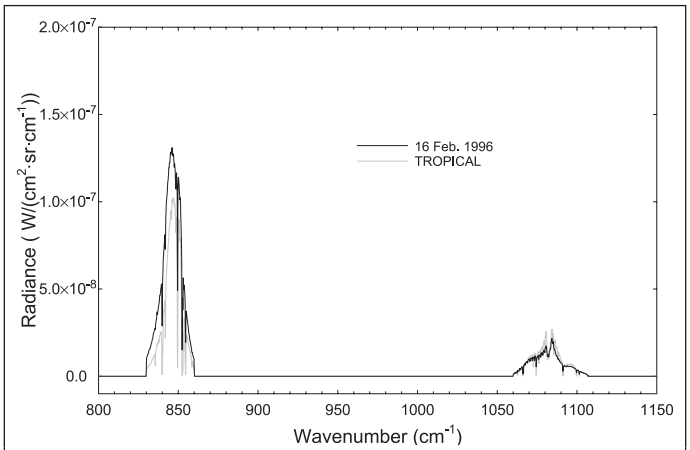

Figure 8. LBLRTM simulations of the downward CFC11 radiance at the surface for two extreme atmospheric scenarios: the cold winter conditions of 16 February 1996, and the warm, humid atmosphere of tropical conditions.

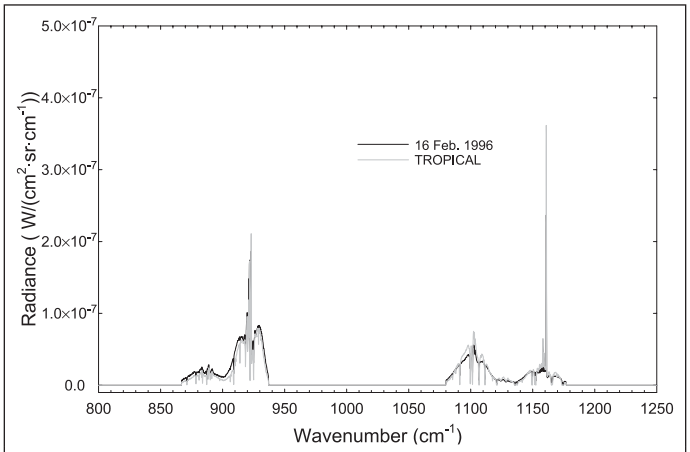

Figure 9. LBLRTM simulations of the downward CFC12 radiance at the surface for two extreme atmospheric scenarios: the cold winter conditions of 16 February 1996, and the warm, humid atmosphere of tropical conditions.

temperature increases and interferes significantly with the bands of all the other radiatively active gases.

Downwelling thermal emission spectra were measured with a ground-based Fourier-transform infrared (FTIR) spectrometer for the cold conditions of 16 February 1996. To determine the fluxes from the measured spectra, LBLRTM was used to simulate the measured thermal emission spectra. The LBLRTM model incorporated radiosonde data, which were subsequently altered slightly in temperature and humidity until agreement was achieved with the measured spectra. The radiance from a particular gas was then extracted by using LBLRTM to simulate the background radiance in the absence of the gas. The corresponding flux for each gas was determined by the same procedure as noted for the LBLRTM simulations. Additional information on the determination of surface radiative fluxes from measured spectra is detailed in the method by Evans and Puckrin (2001).

A summary of the results of the radiative fluxes derived using the column radiation codes of the CCM3, SCAM, and GCM3 climate models and the LBLRTM line-by-line model are shown in **Tables 4–8**. The corresponding absolute flux differences and the percentage flux differences relative to the fluxes derived from the line-by-line model are illustrated for each gas in **Figures 10** and **11**, respectively.

H_2O, CO_2, and H_2O + CO_2

Figure 10A shows that the SCAM results for H_2O are consistently more accurate than those of the other two models for all atmospheric conditions. However, the CCM3 result approaches that of the SCAM H_2O flux for MLS and tropical conditions. The difference in the flux simulated by the GCM3 model becomes progressively larger as the amount of H_2O increases in the atmosphere. From **Figure 11A** it is evident that the CCM3, SCAM, and GCM3 radiation models simulate an H_2O flux that is within 5% of the LBLRTM fluxes, with the exception of H_2O flux calculated for colder atmospheres by the CCM3 code, which is about 10% different.

For CO_2, **Figure 10B** shows that the absolute flux differences for the CCM3 and GCM3 simulations decrease as the H_2O content increases in the atmosphere, whereas the SCAM result tends to oscillate as a function of atmospheric condition. All of the models simulate the CO_2 flux within 2 W/m^2, or about 15% for the worse-case scenario illustrated with the CCM3 and SCAM models for MLS conditions, as shown in **Figure 11B**.

In the case of the radiative flux for combined H_2O + CO_2, **Figure 10C** indicates that the absolute flux difference simulated with the CCM3 and GCM3 codes decreases from a maximum of about 10 W/m^2 to a difference of about 2 W/m^2 as

Table 4. Radiative fluxes (W/m^2) simulated for the conditions of 16 February 1996 using the CCM3, SCAM, and GCM3 radiation models.

Greenhouse gas	NCAR CCM3		SCAM		Canadian GCM3		Measured flux
	Flux	ΔFlux	Flux	ΔFlux	Flux	ΔFlux	
H_2O	102.80	–10.70 (–9.4)	113.40	–0.10 (–0.1)	109.00	–4.50 (–4.0)	113.50
CO_2	29.00	–1.90 (–6.1)	29.50	–1.40 (–4.5)	29.50	–1.40 (–4.5)	30.90
H_2O + CO_2	144.40	–11.00 (–7.1)	155.20	–0.20 (–0.1)	146.80	–8.60 (–5.5)	155.40
CH_4	1.67	+0.65 (+64.0)	1.67	+0.65 (+64.0)	1.19	+0.17 (+17.0)	1.02
N_2O	1.09	–0.10 (–8.4)	1.09	–0.10 (–8.4)	1.93	+0.74 (+62.0)	1.19
O_3	3.56	+0.22 (+6.6)	3.56	+0.22 (+6.6)	3.54	+0.20 (+6.0)	3.34
CFC11	0.11	+0.01 (+10.0)	0.11	+0.01 (+10.0)	0.17	+0.07 (+70.0)	0.10
CFC12	0.23	+0.03 (+15.0)	0.23	+0.03 (+15.0)	0.44	+0.24 (+120.0)	0.20
Total	154.70	–11.30 (–6.8)	165.50	–0.50 (–0.3)	165.50	–0.50 (–0.3)	166.00

Note: ΔFlux is the absolute flux difference between the band model result and the measured result, with the values in parentheses indicating the percentage difference.

Table 5. Radiative fluxes (W/m^2) simulated for MLW conditions using the CCM3, SCAM, and GCM3 radiation models.

Greenhouse gas	NCAR CCM3		SCAM		Canadian GCM3		LBLRTM flux
	Flux	ΔFlux	Flux	ΔFlux	Flux	ΔFlux	
H_2O	148.50	–8.70 (–5.5)	155.50	–1.70 (–1.1)	149.30	–7.90 (–5.0)	157.20
CO_2	24.70	–1.50 (–5.7)	25.30	–0.90 (–3.4)	25.00	–1.20 (–4.6)	26.20
H_2O + CO_2	201.60	–8.40 (–4.0)	208.70	–1.30 (–0.6)	202.10	–7.90 (–3.8)	210.00
CH_4	1.72	+0.75 (+77.0)	1.72	+0.75 (+77.0)	1.27	+0.30 (+31.0)	0.97
N_2O	1.13	+0.16 (+16.0)	1.13	+0.16 (+16.0)	1.82	+0.85 (+88.0)	0.97
O_3	3.41	+0.34 (+11.0)	3.42	+0.35 (+11.0)	3.41	+0.34 (+11.0)	3.07
CFC11	0.13	+0.02 (+18.0)	0.13	+0.02 (+18.0)	0.19	+0.08 (+73.0)	0.11
CFC12	0.27	+0.03 (+13.0)	0.27	+0.03 (+13.0)	0.48	+0.24 (+100.0)	0.24
Total	214.00	–8.90 (–4.0)	221.10	–1.80 (–0.8)	220.80	–2.10 (–0.9)	222.90

Note: ΔFlux is the absolute flux difference between the band model result and the LBLRTM result, with the values in parentheses indicating the percentage difference.

Table 6. Radiative fluxes (W/m^2) simulated for average global conditions using the CCM3, SCAM, and GCM3 radiation models.

Greenhouse gas	NCAR CCM3		SCAM		Canadian GCM3		LBLRTM flux
	Flux	ΔFlux	Flux	ΔFlux	Flux	ΔFlux	
H_2O	198.60	–6.10 (–3.0)	203.40	–1.30 (–0.6)	195.60	–9.10 (–4.4)	204.70
CO_2	21.80	–1.60 (–6.8)	22.10	–1.30 (–5.6)	22.30	–1.10 (–4.7)	23.40
$H_2O + CO_2$	264.60	–5.80 (–2.1)	269.60	–0.80 (–0.3)	264.40	–6.00 (–2.2)	270.40
CH_4	1.89	+0.91 (+93.0)	1.89	+0.91 (+93.0)	1.37	+0.39 (+40.0)	0.98
N_2O	1.22	+0.29 (+31.0)	1.22	+0.29 (+31.0)	2.03	+1.10 (+118.0)	0.93
O_3	3.40	+0.46 (+16.0)	3.41	+0.47 (+16.0)	3.36	+0.42 (+14.0)	2.94
CFC11	0.14	+0.03 (+27.0)	0.13	+0.02 (+18.0)	0.20	+0.09 (+82.0)	0.11
CFC12	0.30	+0.06 (+25.0)	0.30	+0.06 (+25.0)	0.50	+0.26 (+108.0)	0.24
Total	279.60	–7.00 (–2.4)	284.50	–2.10 (–0.7)	284.90	–1.70 (–0.6)	286.60

Note: ΔFlux is the absolute flux difference between the band model result and the LBLRTM result, with the values in parentheses indicating the percentage difference.

Table 7. Radiative fluxes (W/m^2) simulated for MLS conditions using the CCM3, SCAM, and GCM3 radiation models.

Greenhouse gas	NCAR CCM3		SCAM		Canadian GCM3		LBLRTM flux
	Flux	ΔFlux	Flux	ΔFlux	Flux	ΔFlux	
H_2O	255.90	+0.80 (+0.3)	256.80	+1.70 (+0.7)	245.80	–9.30 (–3.6)	255.10
CO_2	7.96	–1.38 (–15.0)	8.03	–1.31 (–14.0)	8.68	–0.66 (–7.1)	9.34
$H_2O + CO_2$	329.60	+1.40 (+0.4)	330.40	+2.20 (+0.7)	326.50	–1.70 (–0.5)	328.20
CH_4	1.42	+0.85 (+149.0)	1.42	+0.85 (+149.0)	1.09	+0.52 (+91.0)	0.57
N_2O	0.97	+0.36 (+59.0)	0.97	+0.36 (+59.0)	1.46	+0.85 (+139.0)	0.61
O_3	3.21	+0.45 (+16.0)	3.21	+0.45 (+16.0)	3.43	+0.67 (+24.0)	2.76
CFC11	0.096	+0.027 (+39.0)	0.096	+0.027 (+39.0)	0.170	+0.100 (+146.0)	0.069
CFC12	0.25	+0.07 (+39.0)	0.25	+0.07 (+39.0)	0.42	+0.24 (+133.0)	0.18
Total	347.90	+1.20 (+0.3)	348.40	+1.70 (+0.5)	347.50	+0.80 (+0.2)	346.70

Note: ΔFlux is the absolute flux difference between the band model result and the LBLRTM result, with the values in parentheses indicating the percentage difference.

Table 8. Radiative fluxes (W/m^2) simulated for tropical conditions using the CCM3, SCAM, and GCM3 radiation models.

Greenhouse gas	NCAR CCM3		SCAM		Canadian GCM3		LBLRTM flux
	Flux	ΔFlux	Flux	ΔFlux	Flux	ΔFlux	
H_2O	294.90	+0.30 (+0.1)	296.10	+1.50 (+0.5)	284.20	–10.40 (–3.5)	294.60
CO_2	4.65	–0.72 (–13.0)	4.71	–0.66 (–12.0)	4.82	–0.55 (–10.0)	5.37
$H_2O + CO_2$	370.90	–2.20 (–0.6)	374.90	+1.80 (+0.5)	371.00	–2.10 (–0.6)	373.10
CH_4	1.20	+0.82 (+216.0)	1.20	+0.82 (+216.0)	0.84	+0.46 (+121.0)	0.38
N_2O	0.81	+0.32 (+65.0)	0.81	+0.32 (+65.0)	1.20	+0.71 (+145.0)	0.49
O_3	1.88	+0.20 (+12.0)	1.90	+0.22 (+13.0)	2.17	+0.49 (+29.0)	1.68
CFC11	0.062	+0.017 (+38.0)	0.063	+0.018 (+40.0)	0.120	+0.075 (+167.0)	0.045
CFC12	0.19	+0.06 (+46.0)	0.19	+0.06 (+46.0)	0.35	+0.22 (+169.0)	0.13
Total	389.10	–2.30 (–0.6)	393.20	+1.80 (+0.5)	392.00	+0.60 (+0.2)	391.40

Note: ΔFlux is the absolute flux difference between the band model result and the LBLRTM result, with the values in parentheses indicating the percentage difference.

the atmosphere becomes warmer and more humid, whereas the SCAM difference is relatively uniform and varies by about 2 W/m^2.

CH_4, N_2O, and O_3

Figures 10D, **10E**, **11D**, and **11E** show that the simulated flux results for CH_4 and N_2O from all three climate codes can be inaccurate by as much as 200%. As a percentage difference, the accuracy in the flux decreases as the temperature and humidity increases in the atmosphere. For CH_4, the CCM3 and SCAM models give identical results, which are about two to three times larger than the corresponding flux calculated with the GCM3 model. Interestingly, this situation is nearly reversed for N_2O, where the CCM3 and SCAM results are about two to three times more accurate than the GCM3 prediction. At first glance it would appear that the absorption bands of CH_4 and N_2O are reversed in one of the models. To determine the origin

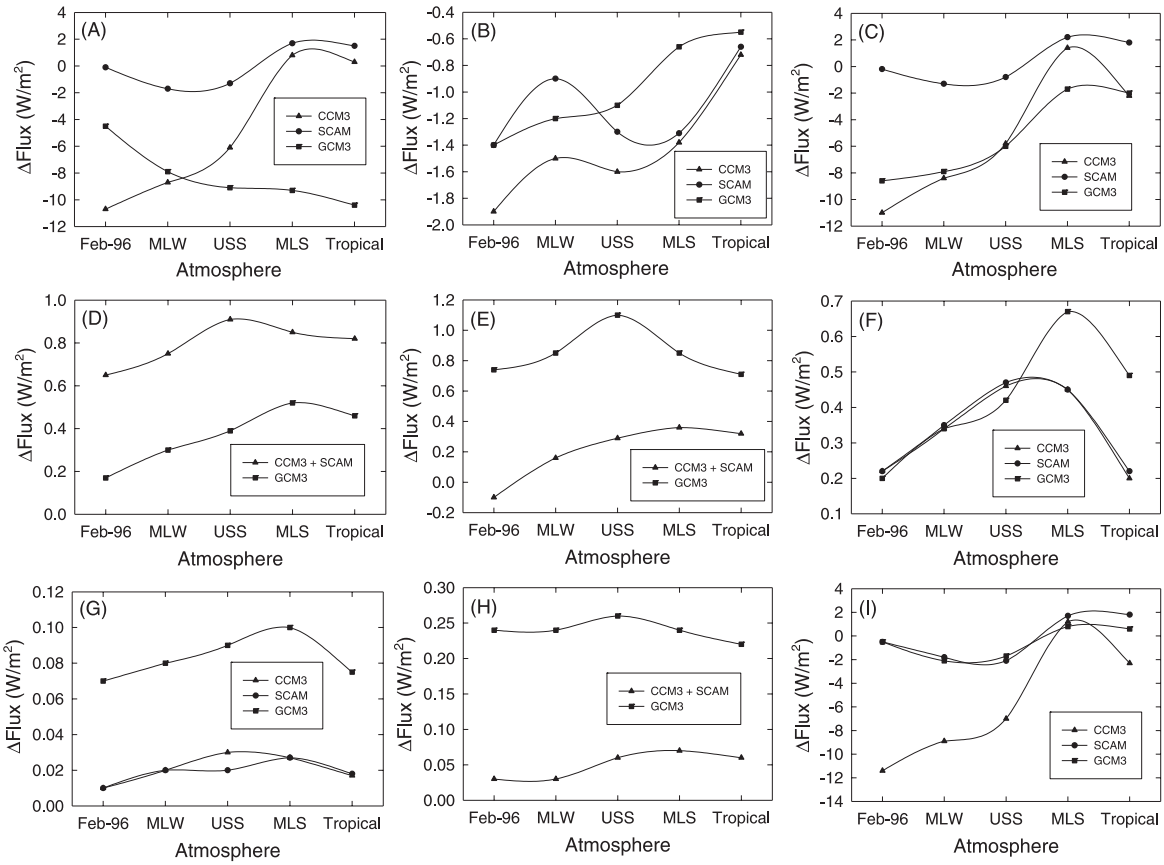

Figure 10. Absolute errors in the radiative fluxes simulated with the radiation codes of the NCAR CCM3 and SCAM models and the Canadian GCM3 model for (A) H_2O, (B) CO_2, (C) $H_2O + CO_2$, (D) CH_4, (E) N_2O, (F) O_3, (G) CFC11, (H) CFC12, and (I) all gases combined. The LBLRTM model was used to calculate the reference fluxes.

of the discrepancy in these results, the SCAM and LBLRTM were used to simulate the downward surface flux for CH_4 using an MLS atmosphere comprising only CO_2, O_3, and the chlorofluorocarbons. This results in a simulation of the CH_4 radiative flux in the absence of H_2O and N_2O gases that have strongly overlapping bands with CH_4. The results, shown in **Table 9**, indicate that the two simulations are in excellent agreement, being different by only 2.3%. This suggests that when a complete atmosphere is present, the overlap of bands affects the calculation of the CH_4 flux adversely. To determine which of the interferents is responsible for the problem, the SCAM and LBLRTM models were used to simulate the flux of CH_4 for an MLS atmosphere containing all gases except H_2O. The results, shown in **Table 9**, indicate that there is a 30% discrepancy in the CH_4 flux simulated with the two models when no H_2O is included in the atmosphere. When the same simulation is repeated for an MLS atmosphere containing all gases except N_2O, there is a 27% error in the CH_4 flux simulated with the SCAM model. This indicates that the effect of the overlap of H_2O and N_2O bands on CH_4 is not adequately modelled.

The O_3 fluxes simulated by the CCM3 and SCAM codes are essentially identical for all atmospheres, and they vary by 5%–15% from the line-by-line value. The GCM3 simulation provides a similar result for all atmospheres up to and including the USS atmosphere; for more humid atmospheres, the GCM3 result nearly doubles in error to about 30%.

CFC11 and CFC12

Although the differences in the absolute CFC fluxes simulated with the climate models are small, they are also among the most inaccurate on a percentage difference basis, as shown in **Figures 10G**, **10H**, **11G**, and **11H**. The CCM3 and SCAM codes model the CFC11 and CFC12 fluxes to within about 0.02–0.06 W/m^2 for all atmospheres; however, this represents a percentage difference of up to 50%. For the simulations performed with the GCM3 model, the error in the CFC11 and CFC12 fluxes can be as large as 170% for the tropical atmosphere. The origin of this disagreement is not obvious; however, owing to the lack of overlapping bands from other gases, the problem is likely related to an inadequate treatment of the CFC absorption bands in the radiation schemes of the climate models.

All gases

As shown in **Figures 10I** and **11I**, the SCAM and GCM3 models simulate the total radiative flux for all gases combined

to within ±2 W/m^2, or 1% on a percentage difference scale. In the case of the CCM3 model, there is a difference of about 12 W/m^2 (or 7%) for the cold conditions of 16 February 1996. The discrepancy improves for the other atmospheres to the point where all three codes give similar results for MLS conditions.

Conclusions

Radiative surface fluxes for several important gases were simulated with the radiation band models from the NCAR CCM3 and SCAM climate models and the Canadian GCM3 climate model. These results were compared with the measured fluxes for very cold winter conditions and with the simulated results for other standard atmospheres using the line-by-line code LBLRTM. The comparison showed that the total surface radiative flux contributed by all the greenhouse gases combined was well simulated by the NCAR SCAM and Canadian GCM3 radiation band models. The two models generally agreed within about 1% of the line-by-line result for all the atmospheric conditions studied. However, the error in the total flux simulated by the older CCM3 code was as much as 7%, depending on the atmospheric conditions. The SCAM code consistently modelled H_2O better than the CCM3 and GCM3 codes, typically displaying errors in the H_2O flux of less than 1 W/m^2 for all atmospheric conditions. All of the models demonstrated significant difficulty in modelling accurately the radiative flux of methane and nitrous oxide. In general, the inaccuracy of these fluxes increased, by as much as 200% in some cases, as the amount of H_2O in the atmosphere increased.

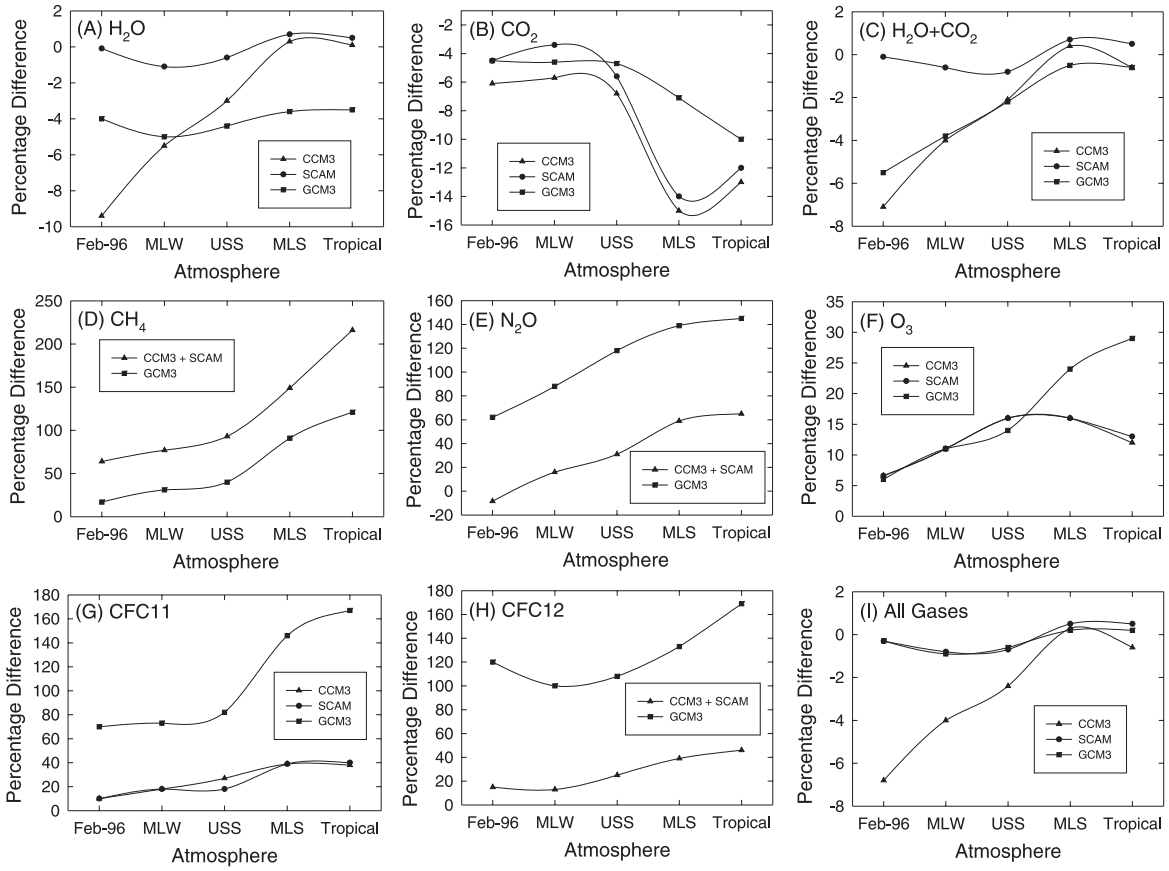

Figure 11. Percentage differences in the radiative fluxes simulated with the radiation codes of the NCAR CCM3 and SCAM models and the Canadian GCM3 model for (A) H_2O, (B) CO_2, (C) $H_2O + CO_2$, (D) CH_4, (E) N_2O, (F) O_3, (G) CFC11, (H) CFC12, and (I) all gases combined. The LBLRTM model was used to calculate the reference fluxes.

Table 9. Simulated radiative fluxes (W/m^2) for methane using the SCAM and LBLRTM radiation models.

Atmosphere	SCAM flux	LBLRTM flux	Percentage difference
MLS atmosphere without H_2O and N_2O	6.18	6.04	2.3
MLS atmosphere without H_2O	6.11	4.69	30.0
MLS atmosphere without N_2O	1.42	1.12	27.0

To explain this inaccuracy, it was demonstrated that overlapping bands of H_2O, CH_4, and N_2O may be poorly represented in the radiation codes of climate models. The CCM3 and SCAM models simulated the CFC fluxes to within 0.06 W/m^2 of the line-by-line result, but this leads to relative errors of 20%–40%. The errors are even larger for the CFCs in the case of the GCM3 model. A comparison of the simulated fluxes derived from the NCAR CCM3 and SCAM radiation models indicates that the latter is significantly more accurate, primarily due to the updated treatment of H_2O emission and absorption and the newer CKD continuum model.

Acknowledgements

We would like to thank NCAR scientists Dr. Charlie Zender and Dr. Jim McCaa, respectively, for making available the CRM model from CCM3 and SCAM, and Jacques Tang for assisting with the compilation of the code. We would also like to thank M. Shephard and S.A. Clough (AER) for the LBLRTM model. Financial support for this work was provided through a grant from the Ontario Research and Development Challenge Fund.

References

Anderson, G.P., Clough, S.A., Kneizys, F.X., Chetwynd, J.H., and Shettle, E.P. 1986. *AFGL atmospheric constituent profiles (0–120 km)*. Optical Physics Division, US Air Force Geophysics Laboratory, Hanscom AFB, Mass. AFGL-TR-86-0110.

Arora, V.K., and Boer, G.J. 2001. The effects of simulated climate change on the hydrology of major river basins. *Journal of Geophysical Research*, Vol. 106, pp. 3335–3348.

Arora, V.K., and Boer, G.J. 2002. A GCM-based assessment of simulated global moisture budget and the role of land-surface moisture reservoirs in processing precipitation. *Climate Dynamics*, Vol. 20, pp. 13–29.

Clough, S.A., and Iacono, M.J. 1995. Line-by-line calculations of atmospheric fluxes and cooling rates 2: Application to carbon dioxide, ozone, methane, nitrous oxide and the halocarbons. *Journal of Geophysical Research*, Vol. 100, pp. 16 519 – 16 535.

Clough, S.A., Kneizys, F.X., and Davies, R.W. 1989. Line shape and the water vapor continuum. *Atmospheric Research*, Vol. 23, pp. 229–241.

Clough, S.A., Iacono, M.J., and Moncet, J.-L. 1992. Line-by-line calculation of atmospheric fluxes and cooling rates: Application to water vapor. *Journal of Geophysical Research*, Vol. 97, pp. 15 761 – 15 785.

Collins, W.D., Hackney, J.K., and Edwards, D.P. 2002. An updated parameterization for infrared emission and absorption by water vapor in the National Center for Atmospheric Research Community Atmosphere Model. *Journal of Geophysical Research*, Vol. 107, Art. 4664.

Ellingson, R.G., Ellis, J., and Fels, S. 1991. The intercomparison of radiation codes used in climate models: Longwave results. *Journal of Geophysical Research*, Vol. 96, pp. 8929–8953.

Evans, W.F.J., and Puckrin, E. 2001. The surface radiative forcing of nitric acid for northern mid-latitudes. *Atmospheric Environment*, Vol. 35, pp. 71–77.

Kiehl, J.T., and Ramanathan, V. 1983. CO_2 radiative parameterization used in climate models: Comparison with narrow band models and with laboratory data. *Journal of Geophysical Research*, Vol. 88, pp. 5191–5202.

Kiehl, J.T., Hack, J.J., Bonan, G.B., Boville, B.A., Briegleb, B.P., Williamson, D.L., and Rasch, P.J. 1996. *Description of the NCAR community climate model (CCM3)*. National Center for Atmospheric Research (NCAR), Boulder, Colo. NCAR Technical Note NCAR/TN-420+STR. 152 pp.

Kiehl, J.T., Jack, J.J., and Hurrell, J.W. 1998. The energy budget of the NCAR Community Climate Model: CCM3. *Journal of Climate*, Vol. 11, pp. 1151–1178.

Luther, F.A., Ellingson, R.G., Fouquart, Y., Fels, S., Scott, N.A., and Wiscombe, W.J. 1988. Intercomparison of radiation codes in climate models (ICRCCM): longwave clear-sky results — a workshop summary. *American Meteorological Society Bulletin*, Vol. 69, pp. 40–48.

Morcrette, J-J. 1991. Radiation and cloud radiative properties in the European centre for medium range weather forecasts forecasting system. *Journal of Geophysical Research*, Vol. 96, pp. 9121–9132.

Philipona, R., Dutton, E.G., Stoffel, T., Michalsky, J., Reda, I., Stifter, A., Wendling, P., Wood, N., Clough, S.A., Mlawer, E.J., Anderson, G., Revercomb, H.E., and Shippert, T.R. 2001. Atmospheric longwave irradiance uncertainty: pyrgeometers compared to an absolute sky-scanning radiometer, AERI, and radiative transfer model calculations. *Journal of Geophysical Research*, Vol. 106, pp. 28 129 – 28 141.

Ramanathan, V., and Downey, P. 1986. A non-isothermal emissivity and absorptivity formulation for water vapour. *Journal of Geophysical Research*, Vol. 91, pp. 8649–8666.

Roberts, R.E., Selby, J.A., and Bibermann, L.M. 1976. Infrared continuum absorption by atmospheric water vapor in the 8–12 μm window. *Applied Optics*, Vol. 15, pp. 2085–2090.

Rothman, L.S., Rinsland, C.P., Goldman, A., Massie, S.T., Edwards, D.P., Flaud, J.-M., Perrin, A., Camy-Peyret, C., Dana, V., Mandin, J.-Y., Schroeder, J., McCann, A., Gamache, R.R., Wattson, R.B., Yoshino, K., Chance, K.V., Jucks, K.W., Brown, L.R., Nemtcinov, V., and Varanasi, P. 1998. The HITRAN molecular spectroscopic database and HAWKS (HITRAN Atmospheric Workstation): 1996 edition. *Journal of Quantitative Spectroscopy and Radiative Transfer*, Vol. 60, pp. 665–710.

Rothman, L.S., Barbe, A., Benner, D.C., Brown, L.R., Camy-Peyret, C., Carleer, M.R., Chance, K., Clerbaux, C., Dana, V., Devi, V.M., Fayt, A., Flaud, J.-M., Gamache, R.R., Goldman, A., Jacquemart, D., Jucks, K.W., Lafferty, W.J., Mandin, J.-Y., Massie, S.T., Nemtchinov, V., Newnham, D.A., Perrin, A., Rinsland, C.P., Schroeder, J., Smith, K.M., Smith, M.A.H., Tang, K., Toth, R.A., Vander Auwera, J., Varanasi, P., and Yoshino, K. 2003. The HITRAN molecular spectroscopic database: edition of 2000 including updates of 2001. *Journal of Quantitative Spectroscopy and Radiative Transfer*, Vol. 82, pp. 5–44.

Shephard, M.W., Goldman, A., Clough, S.A., and Mlawer, E.J. 2003. Spectroscopic improvements providing evidence of formic acid in AERI-LBLRTM validation spectra. *Journal of Quantitative Spectroscopy and Radiative Transfer*, Vol. 82, pp. 383–390.

Wang, J., Anderson, G.P., Revercomb, H.E., and Knuteson, R.O. 1996. Validation of FASCOD3 and MODTRAN3: comparison of model calculations with ground-based and airborne interferometer observations under clear-sky conditions. *Applied Optics*, Vol. 35, pp. 6028–6040.

Zhong, W., and Haigh, J.D. 1995. Improved broadband emissivity parameterization for water vapor cooling rate calculations. *Journal of Atmospheric Science*, Vol. 52, pp. 124–138.